ELASTOHYDRODYNAMICS OF SLOT COATING PROCESS WITH DEFORMABLE ROLL

Danmer Maza Quinones
Department of Mechanical Engineering
Pontifical Catholic University of Rio de Janeiro – PUC-Rio
Rua Marquês de São Vicente 225, Gávea, Rio de Janeiro, Brasil
danmerm@mec.puc-rio.br

Márcio da Silveira Carvalho
Department of Mechanical Engineering
Pontifical Catholic University of Rio de Janeiro – PUC-Rio
Rua Marquês de São Vicente 225, Gávea, Rio de Janeiro, Brasil
msc@mec.puc-rio.br

Abstract. *Slot coating is largely used in the manufacturing process of many products. In general, the minimum thickness that can be coated is proportional to the gap between the coating die and the substrate (usually backed-up by a rigid roll) and inversely proportional to the liquid viscosity. Therefore, in order to obtain thin films with liquid of high viscosity, a very small gap would be necessary. In practice, the clearance between the die and the web has to be large enough to avoid the risk of clashing two hard surfaces. A common solution is the use a backup rolls covered with an elastomeric layer. The liquid in the coating bead develops high enough pressure to deform the resilient cover, which changes the geometry of the flow, characterizing an elastohydrodynamic action. The understanding of the flow is vital to the optimization of this widely used coating method*
The theoretical model presented in this work takes into account the viscous flow, the roll deformation and the free surface effects in order to predict the flow behavior. It consisted of solving the Navier-Stokes equation to describe the free surface flow coupled with an array of springs to model the elastic cover deformation. The equation system was solved by the Galerkin / Finite element method. The resulting set of non-linear algebraic equations was solved by Newton's method. The results indicate how different operating parameters, liquid and roll cover properties affect the flow.

Keywords*: Slot coating, elastohydrodynamics, free boundary problem, finite element method*

1. Introduction

Slot coating is used in the manufacturing process of adhesive and magnetic tapes, specialty papers, imaging films, and many other products. Slot coating belongs to a class of methods known as pre-metered coating: The thickness of the coated liquid layer is set by the prescribed flow rate fed into the coating die and the substrate velocity, and it is independent of the other process variables, making this class of method ideal for high precision coating. In this process, the coating liquid is pumped to a coating die in which an elongated chamber distributes it across the width of a narrow slot through which the flow rate per unit width at the slot exit is made uniform. Exiting the slot, the liquid fills (wholly or partially) the gap between the adjacent die lips and the substrate translating rapidly past them. The liquid in the gap, bounded upstream and downstream by gas-liquid interfaces, or menisci, forms the coating bead, as shown in Fig. 1. The competition between viscous, capillary and pressure forces sets the range of operating parameters in which the viscous free surface flow of the liquid can be two dimensional and steady, which is the desired state. In order to sustain the coating bead at higher substrate speeds, the gas pressure upstream of the upstream meniscus is made lower than ambient, i.e. a slight vacuum is applied to the upstream meniscus (Beguin, 1954).

The region of acceptable coating quality in the space of operating parameters of a coating process is usually referred to as the coating window. Knowledge of coating windows of different coating methods is needed to predict whether a particular method can be used to coat a given substrate at a prescribed production rate. Coating windows can be constructed either from extensive experimentation or from theoretical model.

According to the viscocapillary model developed by Higgins and Scriven (1980), given the substrate speed, the minimum flow rate per unit width - and hence the minimum liquid layer thickness - is set by the greatest adverse pressure gradient that can be created in the downstream part of the gap. The minimum liquid layer thickness ($t_{\min}$) is a function of the capillary number $Ca = \mu V_W / \sigma$ (viscosity and substrate velocity divided by surface tension):

$$\frac{t_{\min}}{H} = \frac{1}{1+1.49Ca^{2/3}}; \quad Ca << 1; \ \mathrm{Re} << 1 \tag{1}$$

Above the critical gap-to-thickness ratio, two-dimensional steady flow cannot exist, according to the viscocapillary flow model. Moreover, the formula indicates that the minimum thickness of liquid that can be coated from a downstream gap of specified clearance is greater, the higher the capillary number. At constant capillary number, the minimum thickness that can be coated is directly proportional to the gap between the coating die and the substrate (usually backed-up by a rigid roll). Therefore, in order to obtain thin films of high viscosity liquid, a very small gap would be necessary. In practice, the clearance between the die and the web has to be large enough to avoid the risk of clashing two hard surfaces. A common solution is the use a backup rolls covered with an elastomeric layer. The liquid in the coating bead develops high enough pressure to deform the resilient cover, which changes the geometry of the flow, characterizing an elastohydrodynamic action.

Several theoretical models have been used to study elastohydrodynamic action in viscous flow. Dowson and Higinson (1966) adopted a simplified elastic deformation model (called the constrained column model), in which the deformation at each point is only a function of the pressure in that location. Then Johnson (1985) proposed that the proportionality constant on the one-dimensional model is a function of the Poisson's ratio ν, the elastic modulus E, and the elastomeric layer thickness film L, and it is given by:

$$K \equiv \frac{P(x)}{\delta(x)} = \frac{(1-\nu)}{(1+\nu)(1-2\nu)}\frac{E}{L} \tag{2}$$

It is clear that this expression cannot be used for incompressible materials, i.e., $\nu = ½$. Dowson and Jin (1989) suggested that the constrained column model (one dimensional model) with the proportionality constant proposed by Johnson can be applied only for Poisson's ratio less than 0.45. If the proportionality constant proposed by Johnson is used to model incompressible materials, the deformation at each point vanishes no matter how large the loading force is.

Coyle (1988) launched theoretical and experimental analysis of the elastohydrodynamics of roll coating. He approximated the behavior of a roll cover by a one-dimensional, linearly elastic model, the same approach used by Dowson and Higginson (1966). Carvalho and Scriven (1999) took up Coyle's analysis and used the one-dimensional spring model coupled with the complete Navier–Stokes formulation for free surface flows and linear stability analysis to study the three-dimensional stability limit of a film-split flow between a rigid and a deformable roll. The results obtained agree qualitatively with experimental evidences on the effect of rubber covered rolls on the behavior of the coating gap.

In this work, the use of deformable back up roll in slot coating process is analyzed by theory. The roll cover deformation is described by the one-dimensional spring model proposed Johnson (1985).

The goal of this work is to analyze the effect of the roll cover deformation on the flow and on the process window.

2. Theoretical model and solution method

The liquid flow between a slot die and a deformable roll is sketched in Fig. 1. The flow in the coating bead is strongly affected by following operating parameters: gap (H), flow rate (Q), web speed (V_W), die configuration and liquids and roll cover properties.

2.1. Equation of the liquid flow and roll cover deformation

Figure 1 shows the liquid domain, bounded by two liquid-air interfaces, the coating die surface and the array of springs that represents the deformable backup roll.

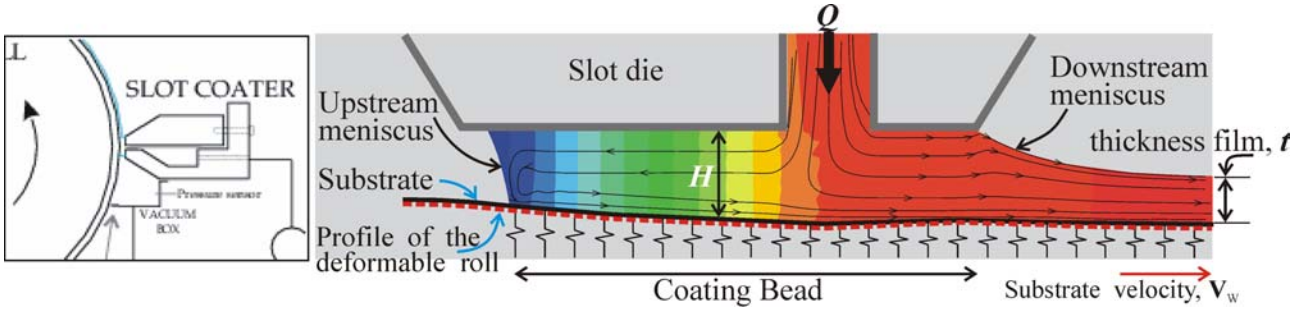

Figure 1. Sketch flow between the slot die and a deformable roll

Coating flows are laminar, and ideally at steady-state and two-dimensional. The motion of the liquid is described by the momentum and continuity equations of incompressible flow:

$$\rho \mathbf{v} \cdot \nabla \mathbf{v} = \nabla \cdot \mathbf{T} \tag{3}$$

$$\nabla \cdot \mathbf{v} = 0 \tag{4}$$

For Newtonian liquid, the stress tensor **T** is given by:

$$\mathbf{T} = \left[-p\mathbf{I} + \mu(\nabla \mathbf{v} + \nabla \mathbf{v}^T) \right] \tag{5}$$

ρ and μ are the density and viscosity of the flowing liquid, e **v** the velocity vector.

2.2. Boundary condition

The boundary conditions are showed in Fig.2:

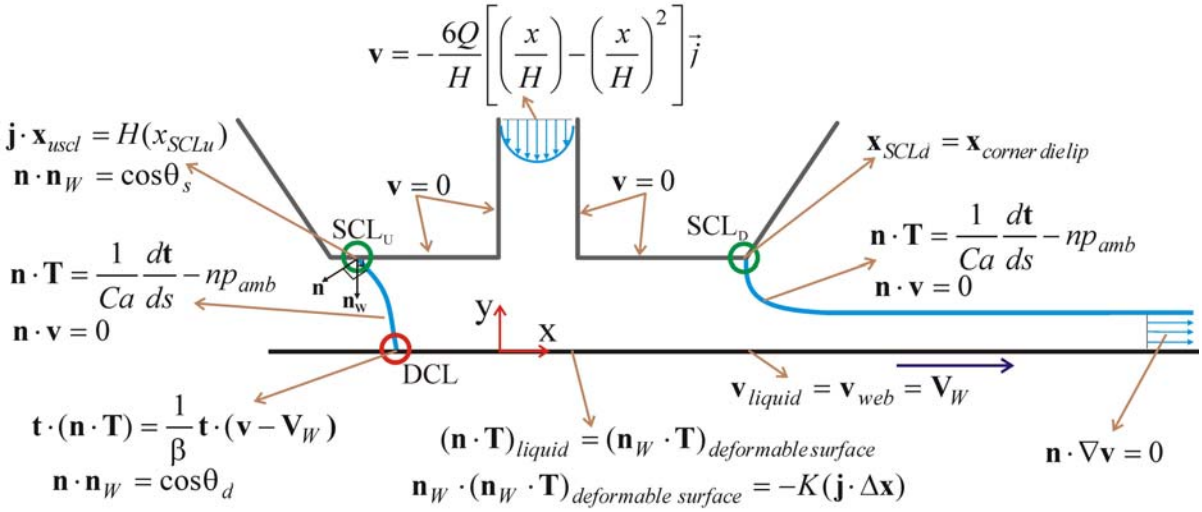

Figure 2. Sketch of the slot coating with boundary conditions for theoretical modeling

The governing equations give rise to a free boundary problem, because the position of the deformable roll surface and the liquid-air interfaces are unknown a priori. The solution method for such problems is recounted briefly here; fuller accounts were given by Kistler and Scriven (1984), Sackinger, Schunk, and Rao (1996), and Carvalho and Scriven (1997).

The important dimensionless parameters are

The Capillary number: $Ca = \frac{\mu V_W}{\sigma}$

Reynolds number: $\mathrm{Re} = \frac{\rho V_W H}{\mu}$

Gap to the feed slot height: $\frac{H}{H_S}$

Elasticity Number: $Ne = \frac{\mu V_W}{K H_S}$, K is the spring constant of the linear spring model

Feed slot height to thickness ratio: $\frac{H_S}{t}$

2.3. Mapping from the physical to reference domain

In order to solve a free-boundary problem using the standard techniques of boundary value problem, the set of differential equations posed in the unknown physical domain Ω has to be transformed to an equivalent set defined in a suitable known reference domain $\overline{\Omega}$, as sketched in Fig. 3. This is done by the mapping $\mathbf{x} = \mathbf{x}(\xi)$ that connects the two domains. Here, the unknown physical domain is parameterized by the position vector $\mathbf{x}$, and the reference domain by ξ. The reference domain adopted is to some extent arbitrary, with the conditions that the boundaries of the reference

domain have to be continuously mapped onto the boundaries of the physical domain and the mapping has to be invertible.

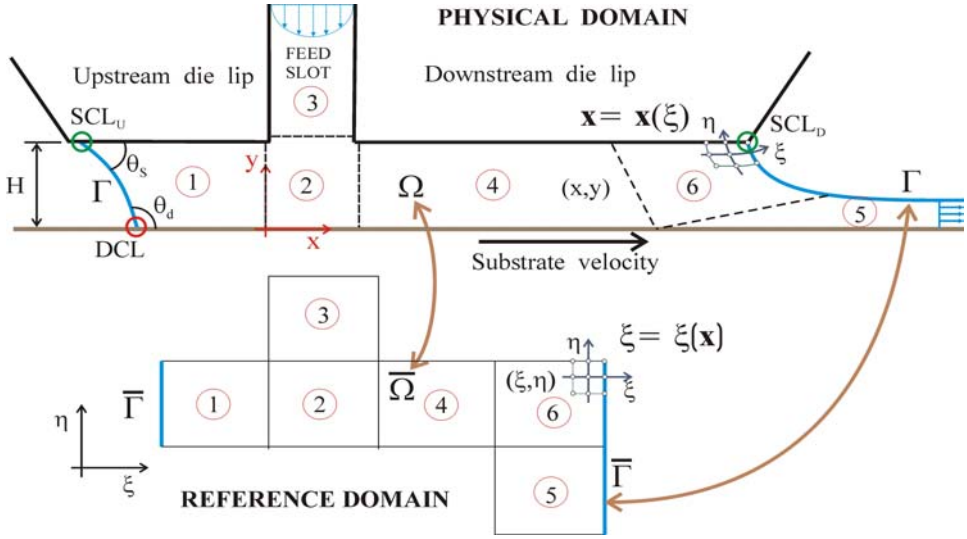

Figure 3. Sketch of mapping from the liquid domain to the reference domain

The mapping used here was presented by de De Santos (1991). He showed that a functional of weighted smoothness can be used successfully to construct the sorts of maps involved here. The inverse of the mapping that minimizes the functional is governed by a pair of elliptic differential equations identical to those encountered in diffusion transport with variable diffusion coefficients. The coordinates ξ and η of the reference domain satisfy:

$$\nabla \cdot D_{\xi} \nabla \xi = 0 \; ; \quad \nabla \cdot D_{\eta} \nabla \eta = 0 \, . \tag{6}$$

The coefficients, D_{ξ} and $D\eta$, control the spacing between the iso-ξ and iso-η coordinates lines (Benjamin et al 1994) of the mesh.

Boundary conditions are needed to solve the second-order partial differential equations. Along solid walls and synthetic inlet and outlet planes, the boundaries are located by imposing a relation between the coordinates from the equation that describes the shape of the boundary and stretching functions are used to distribute the points along the boundaries. The gas-liquid interfaces are located by imposing the kinematic condition and the deformable wall is located by imposing the force balance at each spring. The discrete version of the mapping equations are generally referred to as mesh generation equations. Spatial derivatives with respect to coordinates of the physical domain x and y can be written in terms of derivatives with respect to the coordinates of the reference domain ξ and η by using the inverse of the gradient of the mapping:

$$\nabla_x \phi = \mathbf{J_T}^{-1} \nabla_{\xi} \phi \tag{7}$$

where $\mathbf{J_T}$ is the Jacobian of the transformation

2.4. Finite element formulation of the system equations

The system of partial differential equations presented in the previous section is solved by Galerkin's/Finite Element method. The velocity and node position are represented in terms of bi-quadratic basis functions ϕ_j and the pressure with linear discontinuous functions χj:

$$\mathbf{v} = \sum (\mathbf{v}_j \phi_j) \; ; \quad p = \sum (P_j \chi_j) \; ; \quad \mathbf{x} = \sum (\mathbf{x}_j \phi_j) \tag{8}$$

The Galerkin weighted residual of the continuity, momentum and mesh generation (mapping) are given by:

$$\mathbf{R}_c^i = \int_{\overline{\Omega}} (\nabla \cdot \mathbf{v}) \chi_i J_T \, d\overline{\Omega}, \tag{9}$$

$$\mathbf{R}m_x^i = \int_{\bar{\Omega}} \left[\rho\phi_i \left(u\frac{\partial u}{\partial x} + v\frac{\partial u}{\partial y} \right) + \left(\frac{\partial \phi_i}{\partial x} Txx + \frac{\partial \phi_i}{\partial y} Txy \right) \right] J_T d\bar{\Omega} - \int_{\bar{\Gamma}} \phi_i (\mathbf{n}\cdot\mathbf{T})_x \left(\frac{d\Gamma}{d\bar{\Gamma}}\right) d\bar{\Gamma} \tag{10}$$

$$\mathbf{R}m_y^i = \int_{\bar{\Omega}} \left[\rho\phi_i \left(u\frac{\partial v}{\partial x} + v\frac{\partial v}{\partial y} \right) + \left(\frac{\partial \phi_i}{\partial x} Txy + \frac{\partial \phi_i}{\partial y} Tyy \right) \right] J_T d\bar{\Omega} - \int_{\bar{\Gamma}} \phi_i (\mathbf{n}\cdot\mathbf{T})_y \left(\frac{d\Gamma}{d\bar{\Gamma}}\right) d\bar{\Gamma} \tag{11}$$

$$\mathbf{R}x^i = -\int_{\bar{\Omega}} D_\xi \left(\frac{\partial y}{\partial \eta}\frac{\partial \phi_i}{\partial x} - \frac{\partial x}{\partial \eta}\frac{\partial \phi_i}{\partial y}\right) d\bar{\Omega} + \int_{\bar{\Gamma}} D_\xi \frac{1}{J_T}\left(\frac{\partial y}{\partial \eta}\eta_x - \frac{\partial x}{\partial \eta}\eta_y\right)\phi_i \left(\frac{d\Gamma}{d\bar{\Gamma}}\right) d\bar{\Gamma} \tag{12}$$

$$\mathbf{R}y^i = -\int_{\bar{\Omega}} D_\eta \left(\frac{\partial y}{\partial \xi}\frac{\partial \phi i}{\partial x} - \frac{\partial x}{\partial \xi}\frac{\partial \phi i}{\partial y}\right) d\bar{\Omega} + \int_{\bar{\Gamma}} D_\eta \frac{1}{J_T}\left(-\frac{\partial y}{\partial \xi}\eta_x + \frac{\partial x}{\partial \xi}\eta_y\right)\phi_i \left(\frac{d\Gamma}{d\bar{\Gamma}}\right) d\bar{\Gamma} \tag{13}$$

where J_T is the determinant of the jacobian of the transformation.

When the spring model is used to describe the deformation of the roll cover, the force balance at the deformable wall is also applied in an integral way. Along the deformable wall, one of the residuals of the mesh generation equations is replaced by the weighted residual of the normal stress balance:

$$\mathbf{R}m_y^i = \int_{\bar{\Gamma}} \left\{ \frac{1}{K}\mathbf{N}_0 \cdot (\mathbf{n}\cdot\mathbf{T}) + \mathbf{N}_0 \cdot (\mathbf{x} - \mathbf{X}_0) \right\} \delta_i \left(\frac{d\Gamma_{def}}{d\bar{\Gamma}}\right) d\bar{\Gamma} = 0 \tag{14}$$

The weighting functions δ_i are chosen to be displaced Dirac delta functions, such that the residuals along Γ become

$$\mathbf{R}m_y^i = \left\{ \frac{1}{K}\mathbf{N}_0 \cdot (\mathbf{n}\cdot T) + \mathbf{N}_0 \cdot (\mathbf{x} - \mathbf{X}_0) \right\}_\Gamma = 0 \tag{15}$$

T is the total stress tensor and is defined by equation (5); **n** is the unit vector normal to the boundary Γ and $\mathbf{N}_0$ is the unit vector in the direction of each spring.

The system of partial differential equations reduces to simultaneous algebraic equations for the coefficients of the basis functions of all the fields. This set of equations is non-linear and sparse. It was solved by Newton's method, which requires evaluation of the full jacobian matrix.

$$\mathbf{c}^{(k+1)} = \mathbf{c}^{(k)} + \delta\mathbf{c}; \quad \mathbf{J}(\delta\mathbf{c}) = -\mathbf{R}; \quad \mathbf{J}_{ij} = \frac{\partial \mathbf{R}_i}{\partial \mathbf{c}_j}; \tag{16}$$

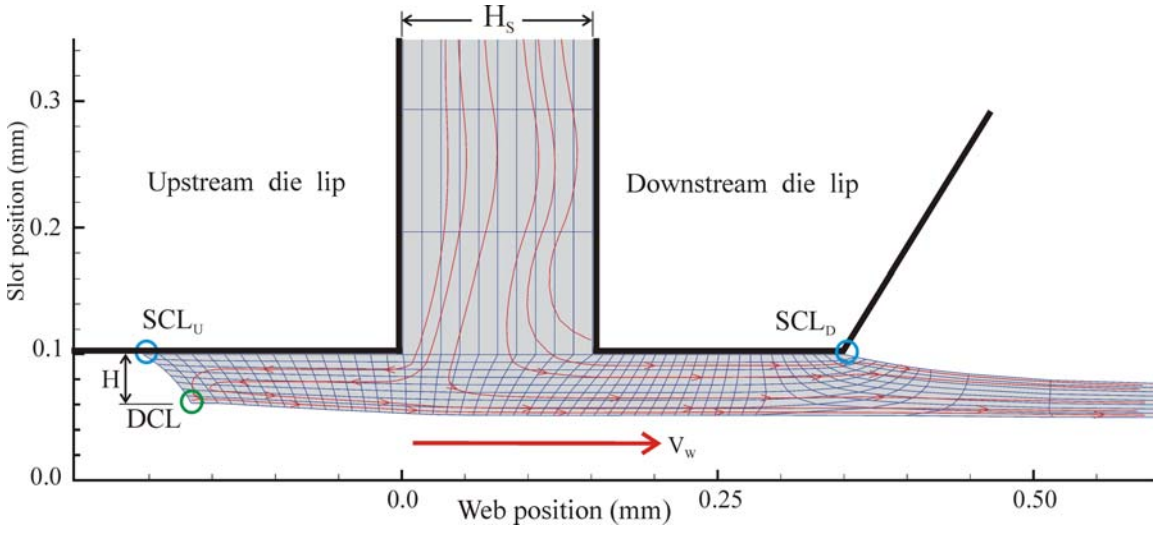

Figure 4. Mesh of the die's geometries

where **c** is the vector of the unknowns coefficient of the basis functions for the velocity, pressure and nodal positions, **R** is the vector of weighted residuals given by above equations. The iteration proceeded until $\|\delta\mathbf{c}\|_2 + \|\delta\mathbf{R}\|_2 \leq \varepsilon$. For each Newton's iteration, a linear system of equations was solved using **LU** decomposition. A pseudo-arc length continuation method coupled with Newton's method was used to automatically construct the entire path of steady states. Figure 4 shows detail of the mesh in the coating bead region.

3. Results

The flow in the coating bead between the slot die and the deformable backup roll was analyzed at different operating conditions.

In the cases analyzed here and in slot coating with deformable roll in general, the bead break up mechanism that leads to a three-dimensional flow is the invasion of the upstream meniscus towards the feed slot as the flow rate falls at a constant web speed, as indicated in Fig.5. The elasticity number was $Ne = 7\times10^{-4}$ and the gap, $H/H_s = 0.33$. The film thickness varied from $H_S/t = 6.0$ up to $H_S/t = 11.6$. Below this value, there is no two-dimensional solution. As the flow rate falls, the pressure under the die becomes smaller and smaller. When the coated thickness is smaller than half the gap, i.e. $H/t > 2$, the pressure under the downstream die lip is below atmospheric, and the roll is pushed up, making the gap smaller than the nominal value, as it is clear from Fig. 5-c''.

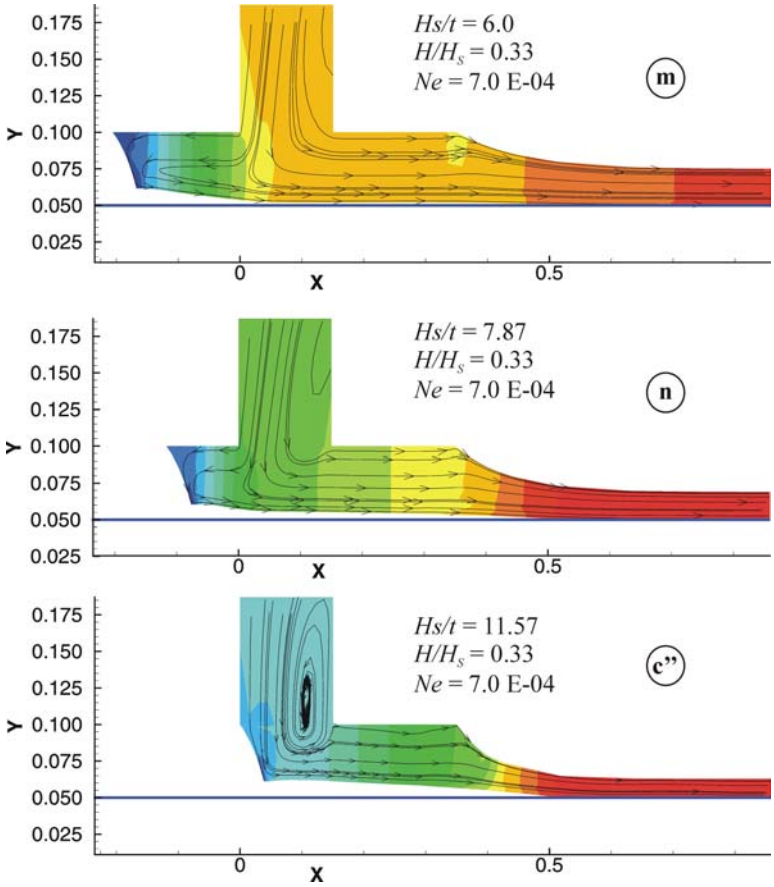

Figure 5: Evolution of the flow states as the film thickness falls.

The minimum film thickness at different gaps and elasticity number is presented in Fig.6. If the slot die and the roll are far apart (large H/H_S) and the elastomeric roll cover has high elastic modulus (low Ne), the pressure that develops in the coating bead is not strong enough to deform the roll surface, the minimum thickness is virtually independent of the roll cover properties and the gap behave as if it were rigid. The minimum film thickness that can be coated falls significantly as the gap is decreased, as expected. At the conditions analyzed in this work, the roll deformation tends to push the limit of the minimum flow rate to smaller values. Figure 7 shows a sequence of flow states at a constant film thickness $H_S/t = 11.6$ and gap $H/H_S = 0.07$ and increasing elasticity number (softer roll cover). As the elastomeric cover becomes softer, the roll deformation increases and the actual gap between the roll and the die become smaller. This geometric variation in the coating gap pushes the upstream meniscus away from the feed slot, stabilizing the flow.

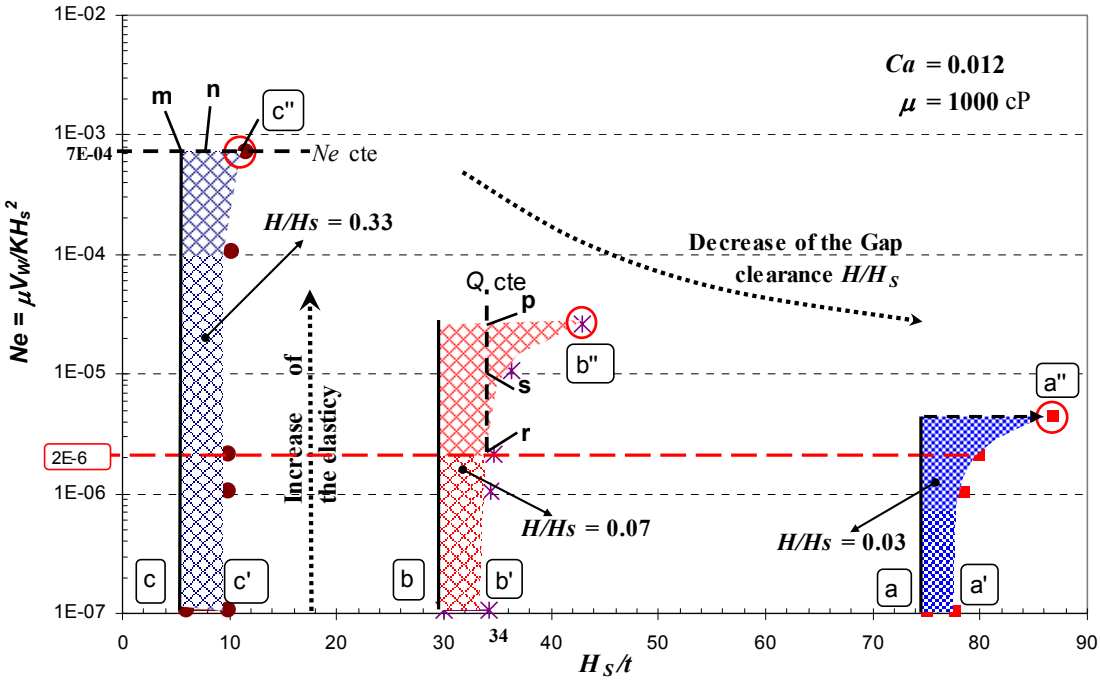

Figure 6. Coating windows: influence of elasticity showed in the plane Ne and the inverse of the film thickness Hs/t.

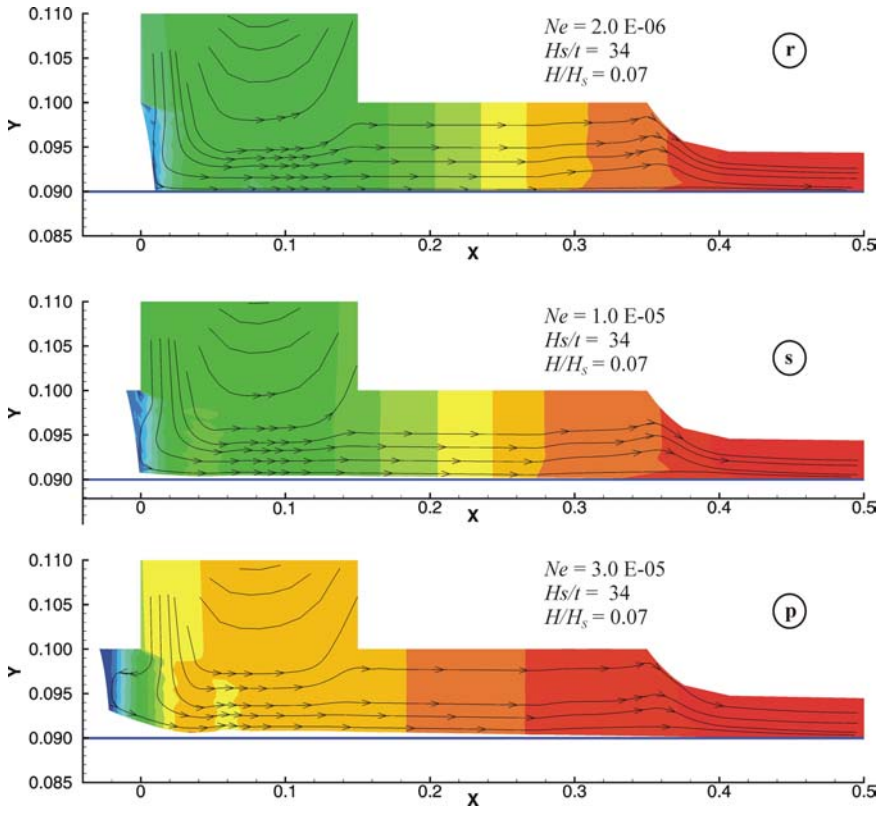

Figure 7: Evolution of the flow in the coating bead as the elasticity number rises (roll cover deformation becomes softer).

The effect of the capillary number on the minimum film thickness is shown in Figure 8. The minimum film thickness falls as the capillary number decreases, i.e. thinner films can be obtained at lower speeds. The effect of the elasticity number at low capillary number and large gaps, e.g. $H/Hs = 0.33$, is opposite to the one discussed before. The reasons for this different behavior are still not clear and it is under investigation.

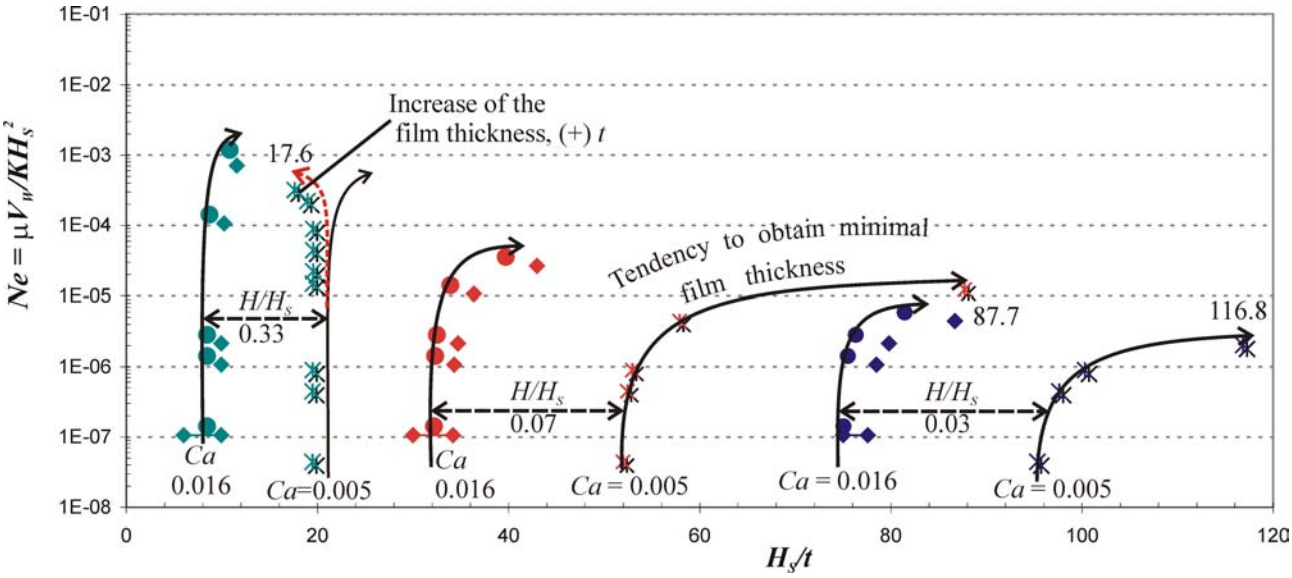

Figure 8. Coating window: influence of the capillary number

4. References

Benjamin, D. F. (1994), "Roll coating flows and multiple rolls systems". PhD Thesis, Univ. of Minnesota, MN, USA.

Beguin, A. L. (1954), "Method of Coating Strip Material", U.S.Pat.2,681,294.

Carvalho, M. S., & Scriven, L. E. (1999). Three-dimensional stability analysis of free surface flows: Application to forward deformable roll coating. Journal of Computational Physics, 150, 534–562.

Carvalho, M. S., & Scriven, L. E. (1997). Flows in forward deformable roll coating gaps: Comparison between spring and plane strain models of roll cover. Journal of Computational Physics, 138(2), 449–479.

Coyle, D.J. (1988a). Experimental studies of flow between deformable rolls. A.I.Ch.E. Spring National Meeting.

Coyle, D. J. (1988b). Forward roll coating with deformable rolls: A simple one-dimensional elastohydrodynamic model. Chemical Engineering Science, 43, 2673.

De Santos, J. M. (1991), "Two-phase cocurrent down flow through constricted passages". PhD Thesis, University of Minnesota, MN, USA.

Dowson, D., & Higginson, G. R. (1966). Elastohydrodynamic lubrication. Oxford: Pergamon Press.

Dowson and Jin (1989). The influence of elastic deformation upon film thickness in lubricated bearing with low elastic modulus coating. Proceedings of the 16th Leeds-Lyon Symposium on Tribology, Lyon, France, pp. 263.

Higgins, B. G. and Scriven, L. E.(1980), "Capillary pressure and viscous pressure drop set bounds on coating bead operatibility", Chemical Engineering Science, 35, 673-682.

Johnson, K. L. (1985). Contact mechanics. Cambridge: Cambridge University Press.

Kistler, S. F., & Scriven, L. E. (1984). Coating flow theory by finite element and asymptotic analysis of the Navier–Stokes system. International Journal for Numerical Methods in Fluids, 4, 207.

Sackinger, P. A., Schunk, P. R., & Rao, R. R. (1996). A Newton-Raphson pseudo-solid domain mapping technique for free and moving boundary problems: A 8nite element implementation. Journal of Computational Physics.

5. Responsibility notice

The authors are the only responsible for the printed material included in this paper.